Coalition of thermo-opto-electric effects in ferroelectrics for enhanced cyclic multi-energy conversion

Gaurav Vats, Jani Peräntie, Jari Juuti, Jan Seidel*, and Yang Bai**

G. Vats, Prof. J. Seidel
School of Materials Science and Engineering, University of New South Wales, Sydney NSW 2052, Australia

Dr. J. Peräntie, Dr. J. Juuti, Dr. Y. Bai
Microelectronics Research Unit, Faculty of Information Technology and Electrical Engineering, University of Oulu, FI-90014 Oulu, Finland

*Corresponding Author: g.vats@unswalumni.com; jan.seidel@unsw.edu.au; yang.bai@oulu.fi

Keywords: KNBNNO, photo-pyro modulation, thermo-opto-electric modulation, cyclic energy conversion, multi-source energy harvesting

Abstract: The concept of multi-source energy harvesting (of light, kinetic and thermal energy) using a single material has recently been proposed. This work discusses the realization of this novel concept, and thus provides insight into electric field-assisted modulation of photocurrent and pyroelectric current in a bandgap engineered ferroelectric KNBNNO ($(K_{0.5}Na_{0.5})NbO_3$-2 mol.% $Ba(Ni_{0.5}Nb_{0.5})O_{3-\delta}$). Thereafter, DC (direct current) electrical modulation under simultaneous inputs of light and thermal changes for photovoltaic and pyroelectric effects, respectively, is utilized to achieve several orders of increase in the output current density. This is attributed to a light-assisted increase in the material's electrical conductivity and ferroelectric photovoltaic effect. The phenomena of electro-optic and thermo-electro-optic DC modulations are further employed to propose two novel energy conversion cycles. The performance of both the proposed energy conversion cycles is compared to that of the Olsen cycle. The electro-optic and thermo-electro-optic cycles are found to harvest 7 and 10 times more energy than the Olsen cycle alone, respectively. Moreover, both energy conversion cycles offer broader flexibility and ease in

operating conditions thus paving a way towards the practical applications of multi-source energy harvesting with a single material for enhanced energy conversion capability and device/system compactness.

1. Introduction

One of the prime reasons for global warming involves the solutions we employ to satisfy our power needs. We are dependent on either conventional such as burning coal and petroleum products or renewable sources of energy such as sunlight, hydropower plants and wind. Moreover, either source of energy requires batteries or other forms of storage facilities, which further leads to environmental pollution and an increased carbon footprint.[1, 2] The problem becomes severe, for instance, in the case of consumer electronics where almost 70 % of the energy is stored using batteries.[2] Therefore, there is an utmost need for self-sustaining consumer electronics.[1, 2] Self-sustaining electronics, which extract energy from surrounding environment to supply their own power need, may help to reduce the dependency on frequent recharging of batteries from external electricity supply by supplementing energy loss occurred during storage and usage. An ideal solution to these aforementioned problems could be a synergized energy harvesting approach from multiple forms of energy such as light (e.g. via photovoltaic effect), mechanical vibrations (e.g. piezoelectric or triboelectric effect) or thermal fluctuations (e.g. pyroelectric or thermoelectric effect) using a device made of a single material,[1-5] or engineered multiple thin layers.[6-9] Consequently, there have been different attempts towards this solution. One concept uses the pyroelectric effect (charge generation due to thermal fluctuations) to support the photovoltaic performance in several materials.[10-12] Recently, light illumination has also been reported for tuning piezoelectric, pyroelectric and dielectric properties.[13-15] Another concept relies on improvement of pyroelectric and/or photovoltaic performance using the piezoelectric effect or thermal biasing.[16-18] In addition, the phenomenon of pyroelectric photodetection is used to develop ultra-fast photodetectors.[19] The energy conversion

capability could be further enhanced if the potentially synergetic multiple energy conversion mechanisms are used in a cyclic manner. Such cycles are documented to enhance the energy conversion using the pyroelectric effect (the Olsen cycle),[20-25] the pyro-magnetic effect,[26-28] and mechanical confinement (enhanced electrical output under mechanical stress).[16, 29, 30] However, the operating ranges of these cycles are constrained due to the involvement of slow thermal, mechanical, and magnetic changes. In this context, two novel energy conversion cycles are proposed in this paper by exploring a novel monolithic multifunctional material - KNBNNO ($(K_{0.5}Na_{0.5})NbO_3$-2 mol.% $Ba(Ni_{0.5}Nb_{0.5})O_{3-\delta}$)).[4, 5, 31]

KNBNNO being a bandgap engineered (1.6 eV) ferroelectric with a good piezoelectric and pyroelectric responses is capable of simultaneously utilizing inputs from an external electric field, stress, thermal fluctuation and light.[4, 5, 31] Recent work has shown optical control of ferroelectric domains[31] and material conductivity in this material. [4, 5, 31] In this paper, we firstly study the DC (direct current) electrical modulation of photocurrent and pyro-current to develop a basic understanding of the material. Thereafter the cumulative effects of the electric field, pyroelectric effect and light illumination are explored. The developed understanding is then utilized to propose two novel energy conversion cycles based on *electro-optic* and *thermo-electro-optic* effects in KNBNNO. The energy conversion performance is finally compared to the Olsen cycle which is well-known for cyclic energy harvesting using the pyroelectric effect.[20-25]

2. Electrical modulation of photo- and pyro-current

Firstly, the macroscopic modulation of photocurrent was studied under the influence of applied DC electric fields. **Figure 1** shows the electrical output under applied (a) positive and (b) negative electric fields of ± 1 to 4 V (equivalent to ± 10-40 V mm^{-1}), measured in dark. The applied DC bias generates currents varying from 25 to 225 nA cm^{-2} as a function of voltage and time. In the case of positive voltages, the current densities appeared to be systematically higher than in the case of

negative voltages. This asymmetry was caused by the external electric field agreeing or contradicting the polarization, which has been studied and discussed elsewhere.[32] Figure 1 (c) shows the photocurrent obtained from KNBNNO corresponding to a laser source of 405 nm wavelength without external electric bias. The photocurrent was induced by the ferroelectric photovoltaic effect. In Figure 1 (d) the photocurrent enhancement by several orders of magnitude can be seen by applying small electric fields. This occurs due to light-assisted tuning of the material conductivity and charges injection due to the ferroelectric photovoltaic effect.[31] The increase in the negative direction is higher in comparison to the positive direction. This asymmetry is due to the poled state of the material as aligned dipoles favor charge collection in one direction but create an internal electric field in the opposite direction resulting in relatively less charge collection.[32] This effect has been used to create e.g. multi-level ferroelectric memory or a photo-detector with a high on-off ratio.[19, 33]

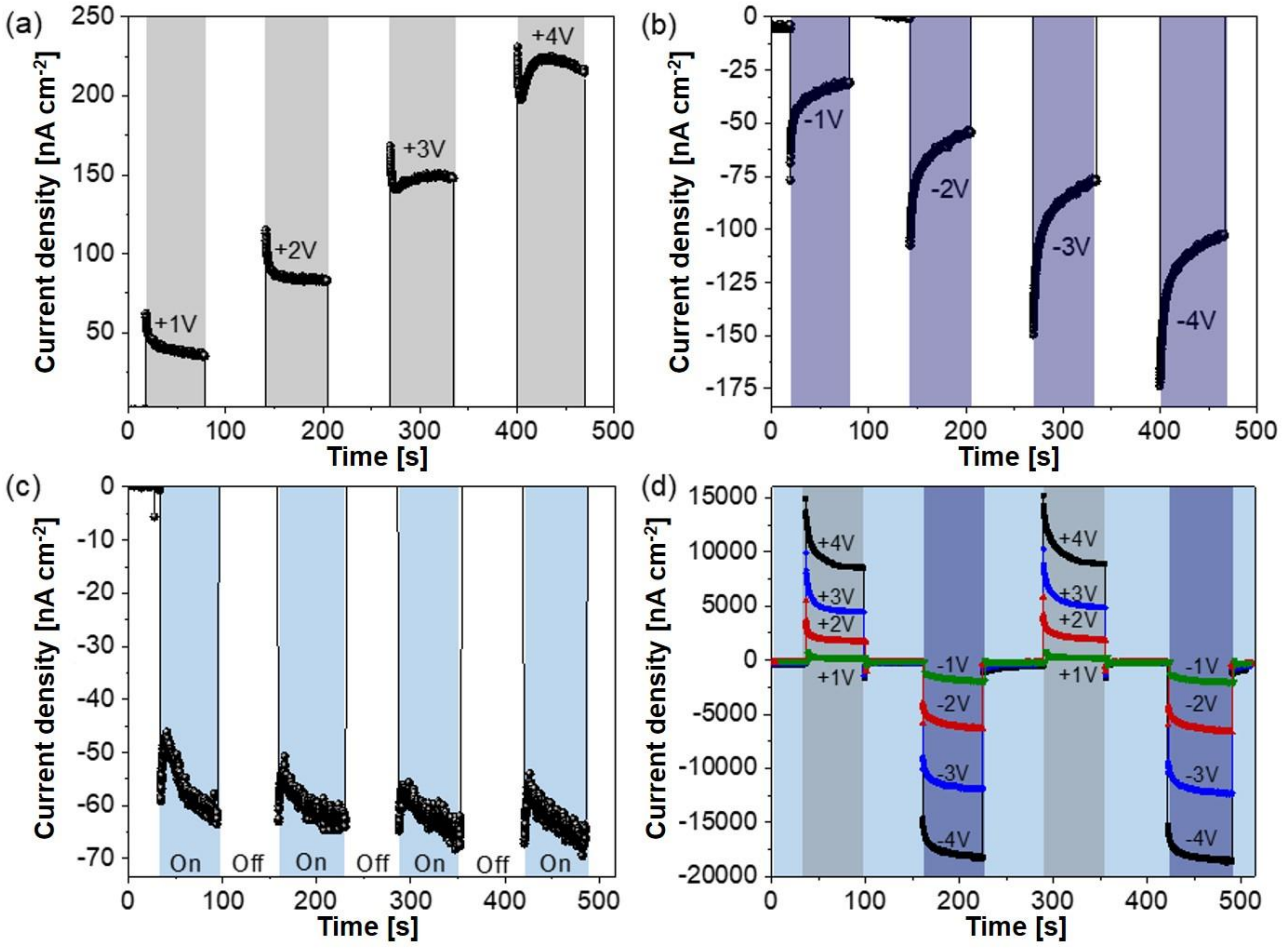

Figure 1. DC electrical modulation of the photocurrent: Electrical current obtained due to applied (a) positive (grey shading) and (b) negative (violet shading) electric bias of 1 V, 2 V, 3 V and 4 V (both (a) and (b) were measured in dark). (c) Photocurrent (sky blue shading) measured in the absence of an applied electric field (light on and off marked). (d) DC electrical modulation of photocurrent (light on) due to applied voltages of ± 1 V, ± 2 V, ± 3 V and ± 4 V.

In the next step, pyro-current was measured for temperature fluctuations of ± 5 °C at 42 °C as shown in **Figure 2** (a). Thereafter, DC electrical modulation of the pyro-current was investigated and is illustrated in Figure 2 for (b) ± 1 V, (c) ± 2 V and (d) ± 3 V. The material was allowed to relax in the absence of the electric field for one cycle after each measurement to avoid modulation due to delay in relaxation of electric field stimulated pyro-current. Grey shaded areas in Figure 2 correspond to the time when a positive DC bias was applied while the negative bias is indicated by the violet shaded area. Although the output of the pyroelectric effect is analogous to an applied AC electric field, the applied positive and negative DC bias caused a respective linear electrical offset in the pyro-current while the magnitude of temperature fluctuation remained the same. Following this, the cumulative effect of electric field and light on pyro-current was investigated. **Figure 3** shows the DC modulation of pyro-current with +4 V (a) in dark and (b) under 405 nm laser. The current collection increase by four orders of magnitudes is a result of the cumulative effect of light-bias and pyroelectric effect. Moreover, the shape of pyro-current collection curve is changed, suggesting that the temperature fluctuation can still affect the charge collection due to cumulative effect of laser exposure and electric field (compare Figure 1 (d) with Figure 3 (b) and Figure 3 (d)). After this, the light and electric field were turned off and the material was allowed to relax (i.e. recover to initial states) merely under temperature fluctuations. An electrical bias of -4 V was applied after 150 s of relaxation and a DC modulation in the pyro-current was noticed as shown in Figure 3 (c). Here, instead of an offset in pyro-current, a continuous decrease in the output is observed. Initially lack of relaxation time before

performing the measurement was envisaged to illustrate such response. However, this was ruled out by repetitive measurements on two different samples by allowing materials to have a relaxation time of more than 30 minutes. Even after a relaxation time of more than 24 hours, the material demonstrated similar behavior. This could only be explained on the basis of a change in the overall state of polarization due to a thermo-electro-optic effect with +4 V and light. Similar behavior could be obtained in multi-level memory storage devices based on ferroelectrics.[34] Still, in the measurement shown in Figure 3 (c) the material was again allowed to relax for one cycle before obtaining pyro-electro-optic modulation with -4 V so as to have least contribution from the trapped current. Again, a significant leap in offset current and current density was observed, and three orders of increase in the magnitude of pyro-current suggests that the process can be used to have enhanced energy conversion or electrical output.

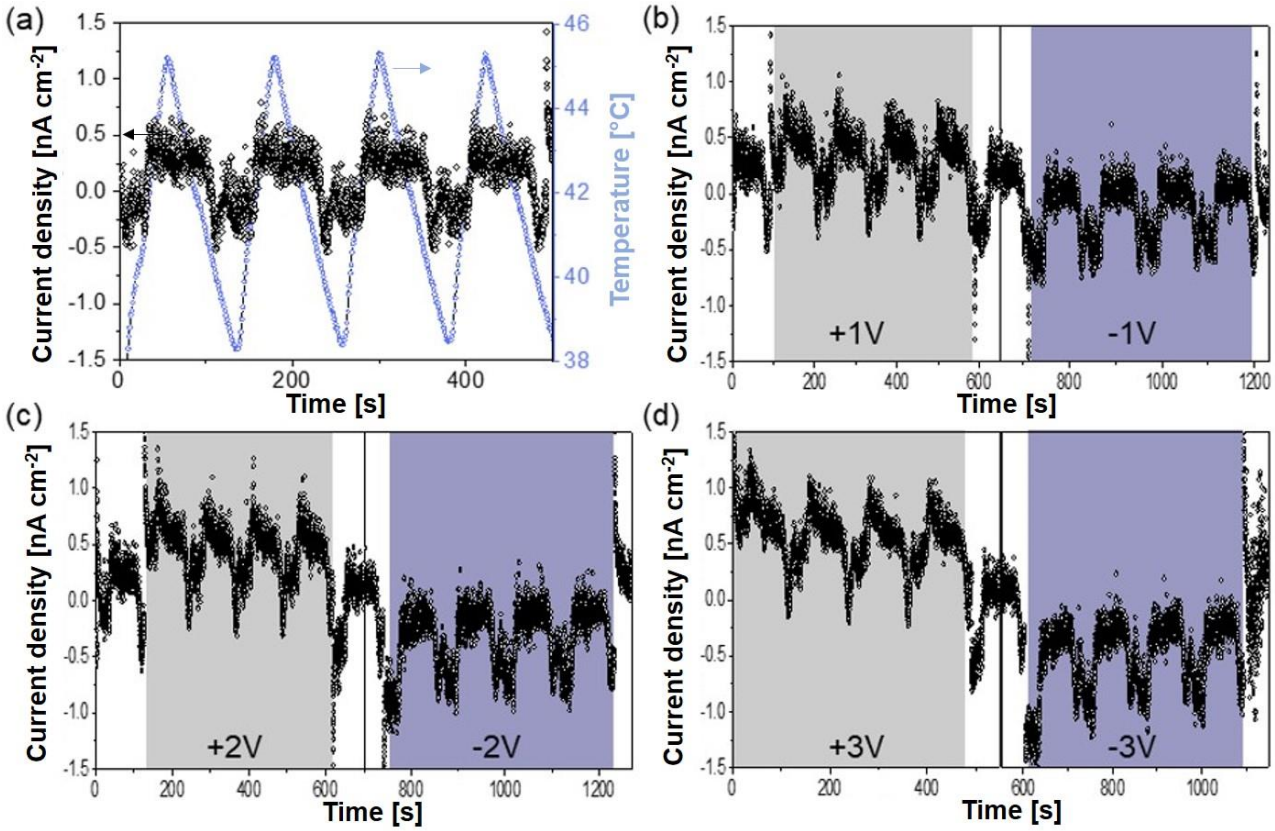

Figure 2. DC electrical modulation of the pyro-current: (a) Pyro-current and the temperature

profile for which the pyro-current is measured. DC modulation of the pyro-current by applied (b) ± 1 V, (c) ± 2 V and (d) ± 3 V (grey shaded areas correspond to applied positive bias; violet shaded areas correspond to the applied negative field).

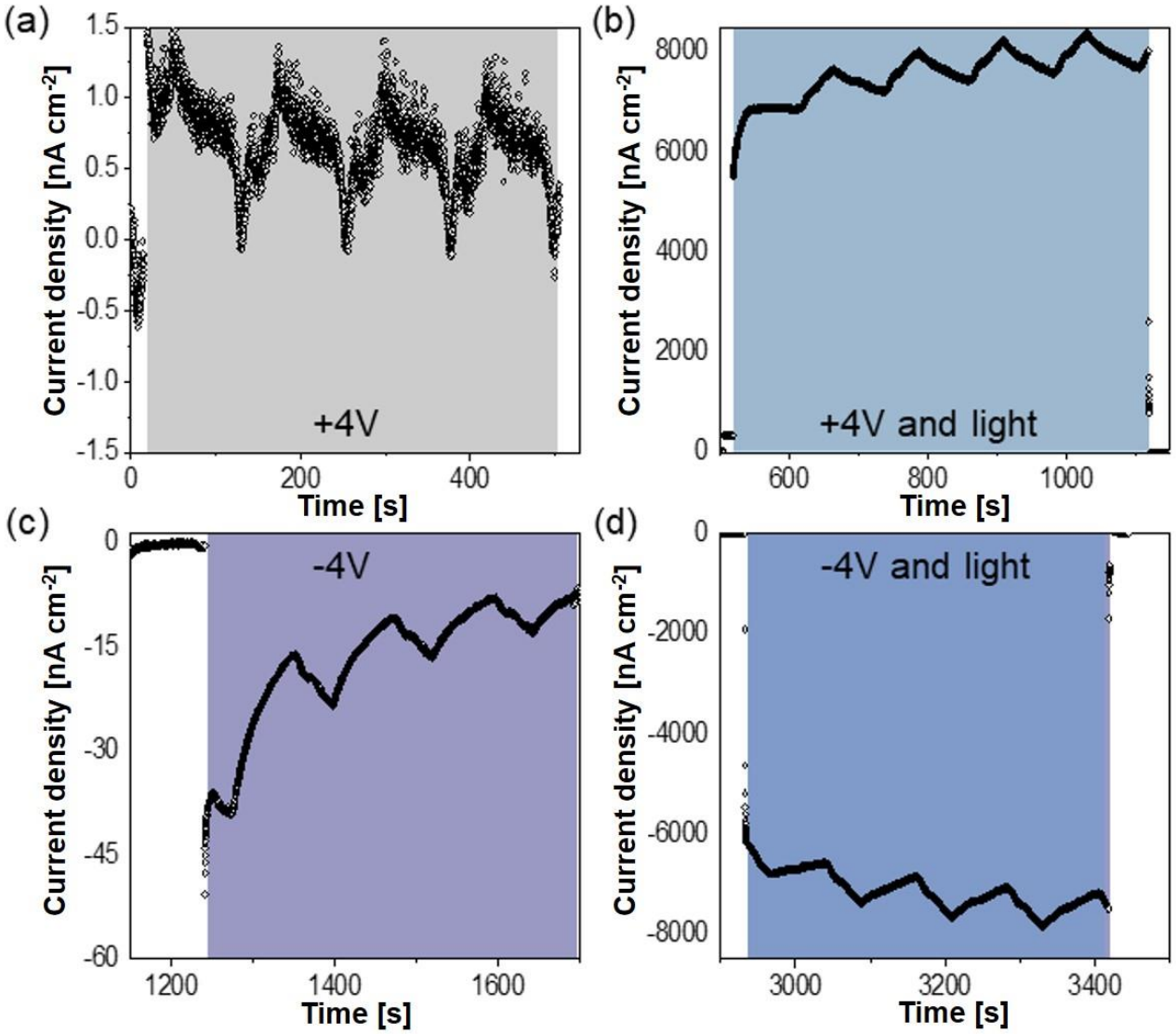

Figure 3. Electro-optic modulation of the pyro-current: (a)(b) Modulation of the pyro-current due to applied +4 V (a) in dark and (b) under 405 nm laser. (c)(d) Modulation of the pyro-current due to applied -4 V (c) in dark and (d) under 405 nm laser.

3. Novel electro-optic and thermo-electro-optic energy conversion cycles

Literature suggests that there exists a method to obtain enhanced energy conversion using the

pyroelectric effect. The method was introduced by R.B. Olsen in 1980s[35-41] and has recently attracted renewed attention[18, 22-24, 30, 42-46] after Vats *et al.* introduced the generalized version of this method for all pyroelectric materials.[20, 25] It is suggested that the material should first be polarized isothermally (at low temperature) and then allowed to exchange heat isoelectrically.[20, 25] The material can then be depolarized isothermally at a higher temperature followed by isoelectric cooling to bring the material at its initial state and to complete the cycle.[20, 25] On a similar platform, here we propose an *'electro-optic cycle'* as shown in **Figure 4** (a), where the isothermal polarization (process *1-2*) of the material takes place and is followed by the isoelectric polarization by the cumulative effect of applied electric field and laser exposure (process *2-3*). Henceforth, the material can be depolarized in the presence of light (process *3-4;* isoillumination) and isoelectric removal of the illumination (process *4-1*) to complete the cycle. The proposed cycle provides an advantage over the Olsen cycle as light-induced changes are fast and comparatively easy to generate. Naturally, this effect becomes more important for optically active ferroelectrics like KNBNNO where only a small or nominal change in polarization occurs over a vast temperature range, as shown in Figure 4 (b) whereas the light-dependent polarization changes are more significant.[31] Moreover, a temperature change could be induced during isoelectric exposure and removal of illumination to further enhance the electrical output, termed a *'thermo-electro-optic cycle'*. However, the *thermo-electro-optic cycle* should be used with caution because the temperature change can induce joule heating (due to thermalization of the charge carriers) which might also cause an increase in the material's resistance, and will, therefore, reduce the overall energy conversion capability.

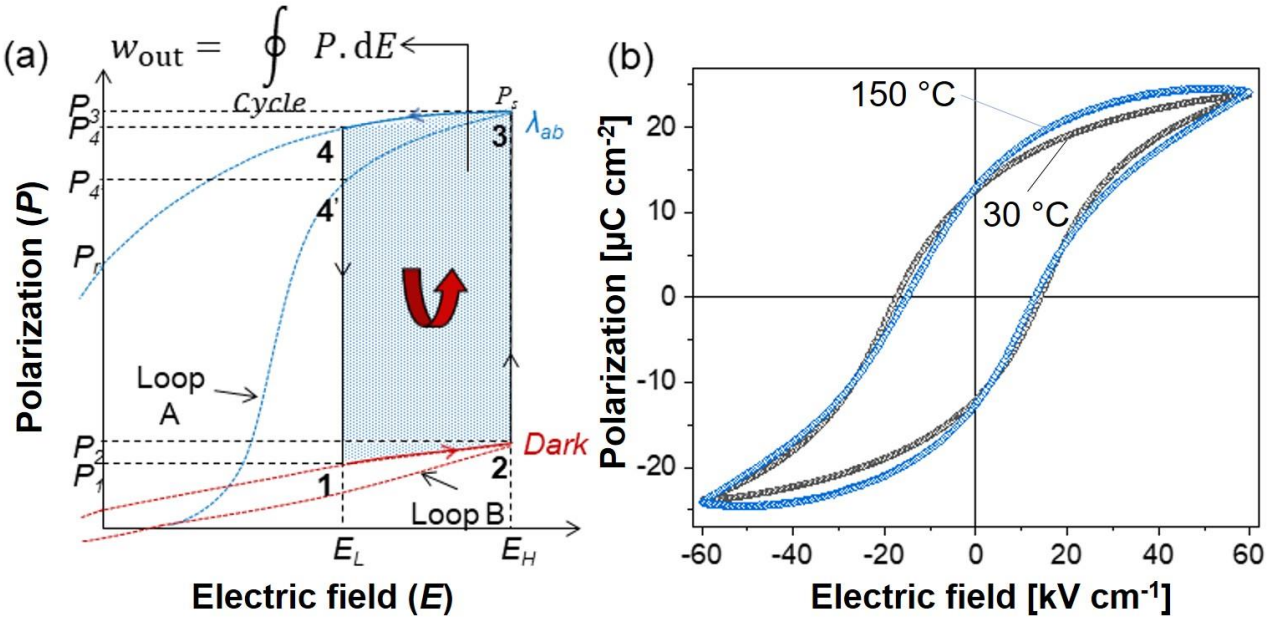

Figure 4. Novel electro-optic energy conversion cycle: (a) Schematic of the novel electro-optic energy conversion cycle with an exaggerated change in polarization with laser exposure of wavelength *(λ_{ab})* (only for indicative purpose). (b) Temperature-dependent *P-E* loops of KNBNNO at 1 Hz to provide an idea of the energy harvesting that could be obtained (from the difference in the area of the upper branches of the two loops) using the Olsen cycle.

To provide a better understanding of this temperature-dependent photocurrent, measurements were performed on KNBNNO as shown in **Figure 5** (a). The photocurrent density in KNBNNO at 20 ˚C was nearly 400 nA cm^{-2}. This increased linearly with an increase in temperature utill 150 ˚C (700 nA cm^{-2}) while decreasing for temperatures higher than 150 ˚C depicted in Figure 5 (b). Interestingly, the photocurrent density at 220 ˚C (350 nA cm^{-2}) is less than the values obtained at 20 ˚C (the Curie temperature of the material is about 400 °C).[5] It is to be noted that the material was maintained at the measured temperature for nearly 30 minutes before performing the photocurrent measurement to avoid any contribution due to the pyroelectric effect. The trend of the temperature dependence of photocurrent could simply be explained on the basis of a change in Fermi-level due to the thermalization of the charge carriers as there are no structural transitions associated with the

investigated temperature range (20 °C to 150 °C). However, there is a rhombohedral to tetragonal structural transition at 170 °C with a nominal change in the lattice parameter.[5] Besides this, no change in the trend for photocurrent was observed at 170 °C (see Figure 5(b)).

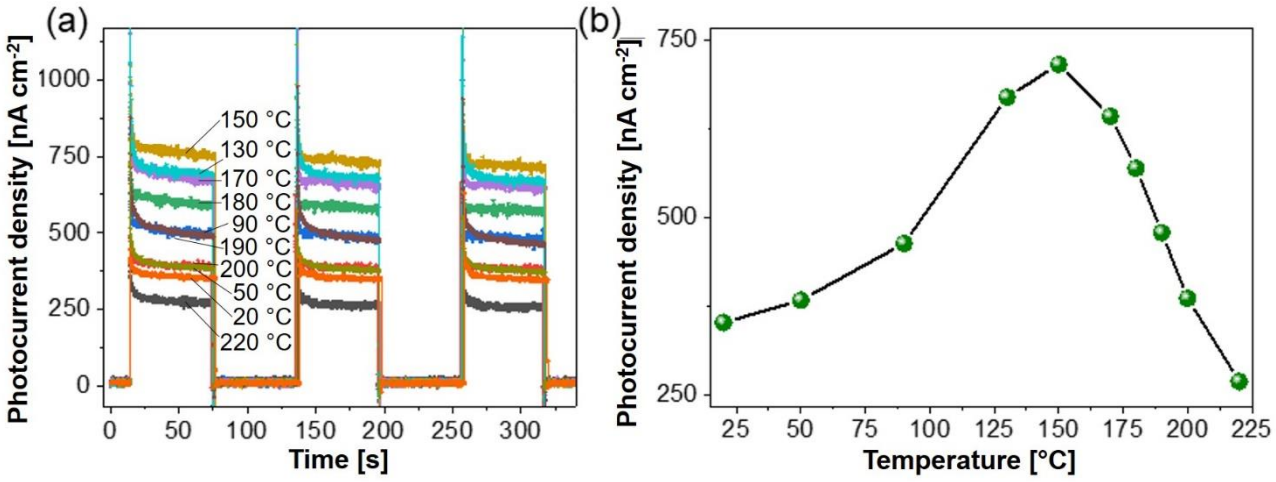

Figure 5. (a) Temperature-dependent photocurrent measurement in the absence of applied electric field; (b) Average value of the photocurrent obtained from Figure 5 (a) as a function of temperature.

4. Comparison of cyclic energy harvesting capabilities

A systematic comparison of cyclic energy conversion efficiency using the Olsen cycle, and novel *electro-optic* as well as *thermo-electro-optic* cycles, was performed by measuring temperature-dependent current-voltage *(I-V)* characteristics of KNBNNO in dark and under illumination with a 405 nm laser source, as shown in **Figure 6** (a) and (b), respectively. These provide a good estimation of the electrical output that could be obtained during isothermal, isoillumination (the process of constant illumination), and isoelectric processes. It also helps to understand that the difference in electrical output obtained during the polarization and depolarization processes is the net work done on the system. From the *I-V* measurements, one can also see that the energy conversion in the last step of isoelectric cooling or photocurrent decay is usually negligible if there is no significant difference in the remanent polarization of the material at positions 4 and 1 in Figure 4 (a). Therefore,

in all energy conversion cycles under investigation, the most important step is *2-3* (isoelectric heating or illumination). From the *I-V* curves depicted in Figure 6, estimated electrical current output from the Olsen (operating temperature range 20-200 °C), and novel electro-optic (operated at 20 °C; in dark or under 405 nm light), as well as thermo-electro-optic cycles (operating temperature range 20-200 °C; in dark or under 405 nm light), are plotted as a function of the applied electric field in **Figure 7**.

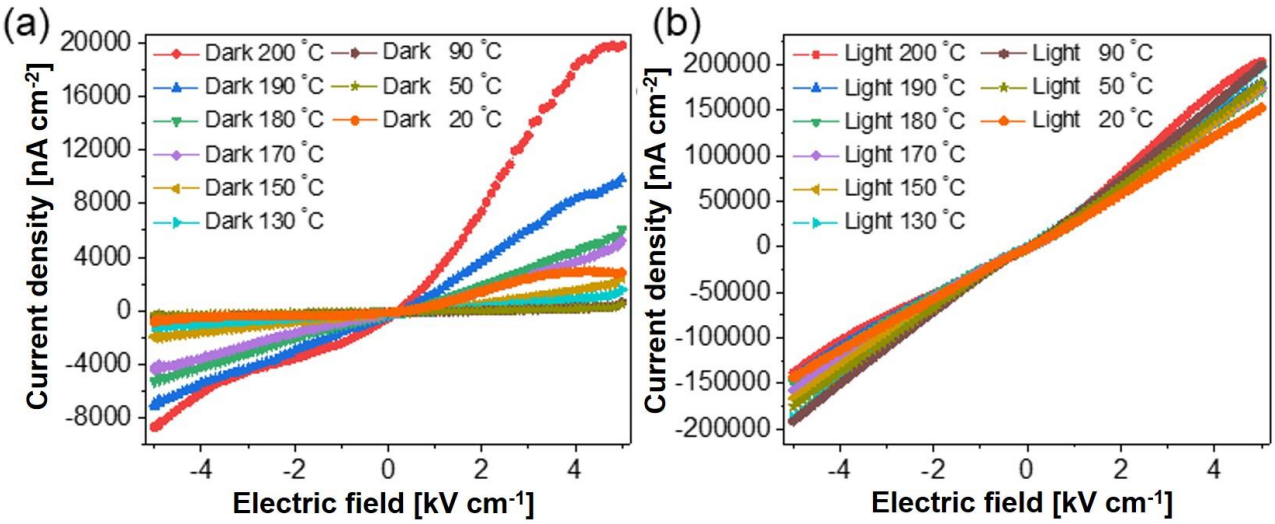

Figure 6. Temperature-dependent *I-V* measurement in (a) dark and (b) under 405 nm laser.

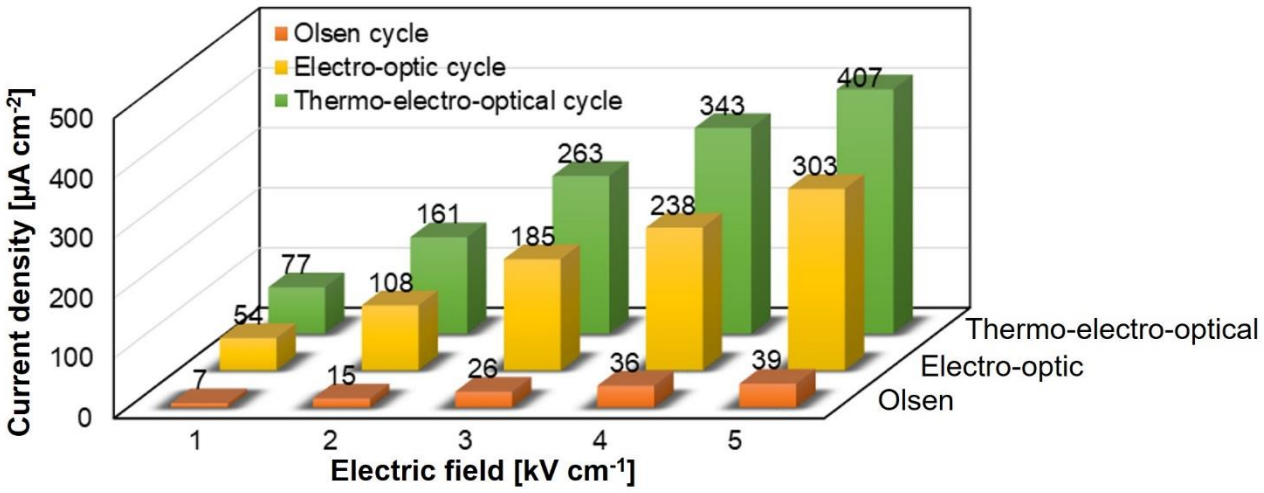

Figure 7. Comparison of the harvested energy using the Olsen cycle (operating temperature range

20-200 °C), novel electro-optic cycle (operated at 20 °C between in dark and under 405 nm laser), and thermo-electro-optic cycle (operating temperature range 20-200 °C; in dark or under 405 nm light).

From the comparison of the harvested electrical energy from the three energy conversion cycles, we infer that in the absence of structural transitions, an optically active ferroelectric can perform significantly better than a material following the classical Olsen cycle. The maximum current density for the Olsen cycle corresponding to electric fields of 0-5 kV cm^{-1} and the operating temperature range of 20 °C to 200 °C was 3.9×10^4 nA cm^{-2}. On the other hand, the novel thermo-electro-optic cycle under the same operating range with a wavelength variation of dark to 405 nm resulted in 4.1×10^5 nA cm^{-2} which is more than 10 times higher when compared to the Olsen cycle. Moreover, the current generation using the electro-optic energy conversion cycle corresponding to the same operating electric field range was 3×10^5 nA cm^{-2} (~ 8 times higher than the Olsen cycle). The highest energy conversion efficiency of the thermo-electro-optic cycle among all three cycles suggests that using a light source can also improve the performance of the Olsen cycle by several orders. Interestingly, the harvested output current using the Olsen cycle for KNBNNO is already ~3.6×10^4 times higher than the pyro-current (compare Figure 7 and Figure 2). Similar observations can be made from the power density calculations shown in Table 1. To manifest the feasibility of all energy conversion cycles under consideration, a comparison of generated electrical power density *(P =* applied voltage *(V)* × obtained current *(I))* output using all cycles with direct output from KNBNNO under normal conditions (without temperature change and laser exposure) at room temperature and at 200 °C is presented in Table 1. The anticipated harvested energy in Table 1 is low due to the low applied low electric fields. However, a significant change in power obtained by the direct application of voltages at 20 °C and 200 °C during all three energy conversion cycles helps to understand the importance of cyclic energy harvesting. Clearly, the power density for the Olsen cycle is higher by a factor of 10 while for thermo-electro-optic cycle is higher by a factor of more than 100. The variation

in direct power density obtained at 20 °C and 200 °C to that of Olsen cycle is not appealing due to the absence of structural transitions. The Olsen cycle is well known to have a high energy conversion if there are any structural transitions occurring in the operating temperature range.[25] The performance under laser illumination is likely to further increase as shown in the presented case of KNBNNO. Importantly, the novel electro-optic energy conversion cycle offers ease of operation, because fast thermal fluctuations are more difficult to achieve than illumination changes. Since the maximum output in the electro-optic cycle is obtained during the process steps *2-3*, it is wise to maintain the material at this step for constant high electrical energy output. In short, this process of obtaining higher photoresponse by applying small electric fields on the material could be a potential solution for improving the photovoltaic performance of ferroelectrics. We hope that the proposed novel energy conversion cycles with the significant improvement compared to conventional conversion cycles attracts the further interest of the scientific community and paves a way for practical applications with improved energy output under multiple energy inputs.

Table 1: Anticipated maximum power density from KNBNNO on direct application of voltages at 20 °C and 200 °C with the Olsen, electro-optic, and thermo-electro-optic cycles.

	Maximum power density $\|P_{max}\|$ [μW cm^{-2}]				
Applied electric bias	Direct power		Olsen cycle	Electro-optic cycle	Thermo-electro-optic cycle
	20 °C	200 °C	20-200 °C	Dark to illumination (405 nm laser) at 20 °C	Dark to illumination (405 nm laser) with heating 20-200 °C
1 V	0.8	2.8	7	54	77
2 V	3.5	14.8	30	216	322
3 V	7.4	38.5	78	555	789
4 V	11.8	73.4	144	952	1372

It is worth pointing out that the light source used in this work was a monochromatic 405 nm (equivalent photon energy 3.06 eV) laser with a power density of about 10 W cm^{-2}. In comparison, the standard AM 1.5G solar spectrum has a broad wavelength distribution (250-2500 nm, equivalent

to 0.5-5 eV photon energy) with an overall power density of 100 mW cm^{-2}. The monochromatic laser was chosen in this work in order to exclude possible heating effect caused by the infrared part of a solar spectrum which could interfere the pyroelectric effect. However, the KNBNNO was sensitive to almost the entire solar spectrum (1.6-5 eV, where most energy lies). Therefore, a more significant coalition effect of the thermo-opto-electric energy conversion coupling can be expected under an actual solar illumination in potentially practical applications.

5. Conclusions

In conclusion, this work presents two novel energy conversion cycles (electro-optic and thermo-electro-optic energy conversion cycles) for optically active ferroelectrics like KNBNNO. The performance of these novel cycles is compared with the well-known pyroelectric energy harvesting Olsen cycle. Both new energy conversion cycles are found to be capable of providing several times higher energy conversion efficiency in contrast to the Olsen cycle alone for KNBNNO, which is likely to be improved further by introducing structural transitions. In addition, the proposed energy conversion cycles provide advantages of ease in operation and more flexibility in operating conditions than the Olsen cycle. The work also provides insight into the DC electrical modulation of photocurrent and pyro-current followed by electro-photo-pyroelectric modulations in KNBNNO, which is also found to demonstrate temperature-dependent variation in the photoresponse attributed to changes in the electronic structure of the material. The presented work is expected to stimulate further research into cyclic energy harvesting by the combined photovoltaic and pyroelectric effects in ferroelectrics.

6. Experimental section

KNBNNO ceramic samples were synthesized via the conventional solid-state route[47] as reported in detail elsewhere. [4, 5, 31] The reactants, K_2CO_3 (CAS 584-08-7, ≥ 99 %, J. T. Baker, USA), Na_2CO_3

(CAS 497-19-8, ≥ 99 %, Sigma-Aldrich, USA), $BaCO_3$ (CAS 513-77-9, 99.98 %, Aldrich Chemistry, USA), NiO (CAS 1313-99-1, 99.999 %, Aldrich Chemistry, USA) and Nb_2O_5 (CAS 1313-96-8, 99.9 %, Aldrich Chemistry, USA), were mixed and then calcined at 850 ˚C for 4 hours. The calcined powder was milled, shaped into disc green bodies, and subsequently sintered at 1165 ˚C for 2 hours. After polishing, the samples were sputtering coated by 200 nm thick Cr-Au electrode on one side and 200 nm thick indium tin oxide (ITO) on the other side as a transparent electrode to let incident light go through. The final dimensions of the samples were 100-120 µm in thickness and 1-2 mm in diameter. The samples were poled at 60 kV cm^{-1} in silicone oil at room temperature and in dark. The poling electric field was provided by a voltage amplifier (Ultravolt, USA). During poling the positive and negative polarities of the voltage amplifier were connected to the ITO and Cr-Au electrodes, respectively, resulting in a net polarization pointing towards the ITO electrode after poling.

Figure 8 explains the measurement setup in schematic and shows a picture of a sample (the ITO side facing upward). The sample was placed on a temperature-controlled stage (LTS 350, Linkam Scientific Instruments, UK). The heating plate of the sample stage did not only provide the heat source but also acted as a bottom conductive contact. Four micropositioners with Au coated tips of a probe station (PVX400, Wentworth Laboratories, UK) connected the sample with a SourceMeter (2450, Keithley, USA) – ‘‘force high’’ and ‘‘sense high’’ to the ITO electrode and ‘‘force low’’ and ‘‘sense low’’ to the heating plate thus the Cr-Au electrode of the sample. A focused 405 nm, 50 mW laser with a beam size of 0.8 ± 0.1 mm in diameter at e^{-2} and a beam quality factor M^2 of < 1.2 (OBIS LX/LS Series, Coherent, USA) was fixed above the sample to provide the light source. For both photocurrent and pyro-current measurements, one pair of the probes (force high and force low) was applying external electric bias and the other pair (sense high and sense low) was collecting the output electric signals (currents). Both the input and output electric signals were recorded by the same source meter using its embedded interface software. The current density was calculated from the entire surface area of the sample. In photocurrent measurement, the source meter kept recording data whilst

the laser was turned on and off. In pyro-current measurement, the source meter kept recording data and the temperature fluctuation profile was programmed and implemented via the temperature control unit of the sample stage. Considering the pyro-current is very sensitive to temperature variation, the sample was made rather small in size as mentioned above in order to minimize heating or cooling lag between temperatures of the sample and the heating plate, and thus to reduce possible errors and noise caused by such a temperature mismatch. In addition, the connection cables between the sample and source meter had a triaxial configuration which helped to suppress possible noise and interference from the environment to the lowest possible level.

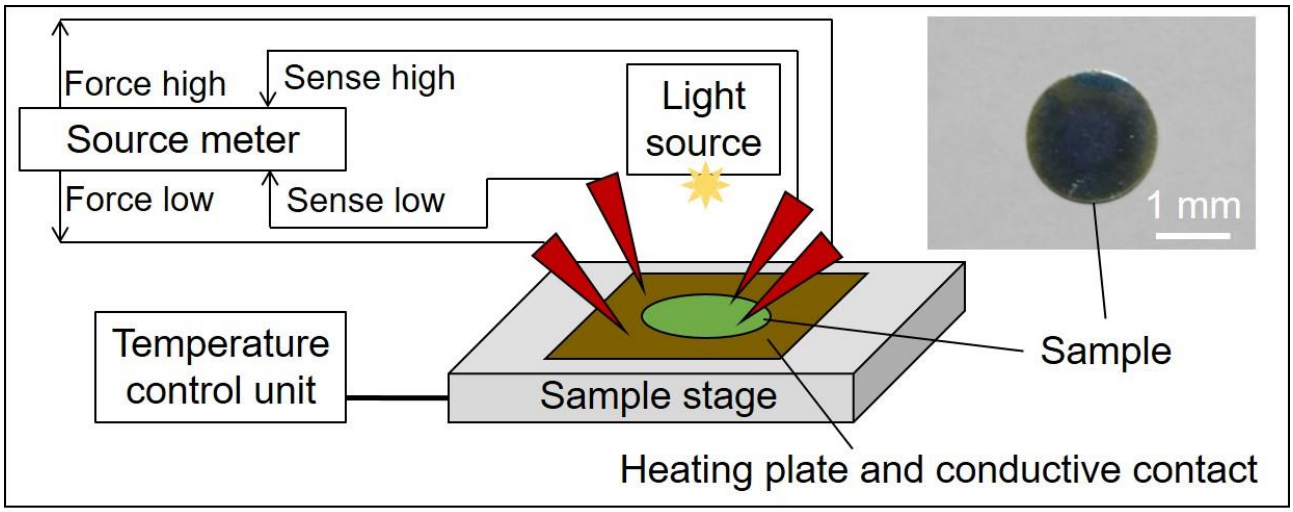

Figure 8. Schematic of the measurement setup for photocurrent and pyro-current, and a picture of the measured sample.

Acknowledgments

The authors acknowledge support from the Australian Research Council (ARC) through Discovery Grants. G.V acknowledges the financial support from the Tiina and Antti Herlin Foundation, Finland. J.P. acknowledges the funding by the Academy of Finland (grant number 298409). Y.B. would like to acknowledge the joint funding by the University of Oulu and Academy of Finland profiling action ‘‘Ubiquitous wireless sensor systems’’ (grant number 24302332). The authors also acknowledge the Centre for Material Analysis of the University of Oulu for the use of their facilities and for the

fabrication of the electrodes.

Conflict of interest

The authors declare no conflict of interest.

References

[1] R. Pandey, G. Vats, J. Yun, C. R. Bowen, A. Ho-Baillie, J. Seidel, K. T. Butler, S. I. Seok, *Adv Mater.* **2019**, *31*, 1807376.
[2] Y. Bai, H. Jantunen, J. Juuti, *Adv Mater.* **2018**, *30*(34), 1707271.
[3] Y. Bai, T. Siponkoski, J. Perantie, H. Jantunen, J. Juuti, *Appl. Phys. Lett.* **2017**, *110*(6), 063903.
[4] Y. Bai, G. Vats, J. Seidel, H. Jantunen, J. Juuti, *Adv Mater.* **2018**, *30*(43), 1803821.
[5] Y. Bai, P. Tofel, J. Palosaari, H. Jantunen, J. Juuti, *Adv Mater.* **2017**, *29*(29), 1700767.
[6] H. Zhang, Y. Xie, X. Li, Z. Huang, S. Zhang, Y. Su, B. Wu, L. He, W. Yang, Y. Lin, *Energy.* **2016**, *101*, 202-210.
[7] H. Zhang, S. Zhang, G. Yao, Z. Huang, Y. Xie, Y. Su, W. Yang, C. Zheng, Y. Lin, *ACS Applied Materials & Interfaces.* **2015**, *7*(51), 28142-28147.
[8] K. Zhang, Z. L. Wang, Y. Yang, *ACS Nano.* **2016**, *10*(11), 10331-10338.
[9] K. Zhang, S. Wang, Y. Yang, *Adv. Energy Mater.* **2017**, *7*(6), 1601852.
[10] A. Katti, R. A. Yadav, *Phys. Lett. A.* **2017**, *381*(3), 166-170.
[11] Q. Jiang, Y. Su, X. Ji, *Phys. Lett. A.* **2012**, *376*(45), 3085-3087.
[12] V. G. Karpov, D. Shvydka, *Phys. Status Solidi-Rapid Res. Lett.* **2007**, *1*(4), 132-134.
[13] M. Coll, A. Gomez, E. Mas-Marza, O. Almora, G. Garcia-Belmonte, M. Campoy-Quiles, J. Bisquert, *Journal of Physical Chemistry Letters.* **2015**, *6*(8), 1408-1413.
[14] H. Borkar, V. Rao, M. Tomar, V. Gupta, J. F. Scott, A. Kumar, *RSC Adv.* **2017**, *7*(21), 12842-12855.
[15] H. Borkar, V. Rao, S. Dutta, A. Barvat, P. Pal, M. Tomar, V. Gupta, J. F. Scott, A. Kumar, *J. Phys. -Condes. Matter.* **2016**, *28*(26), 265901.
[16] I. M. McKinley, S. Goljahi, C. S. Lynch, L. Pilon, *J. Appl. Phys.* **2013**, *114*(22), 224111.
[17] M. Yang, D. J. Kim, M. Alexe, *Science.* **2018**, *360*(6391), 904-907.
[18] G. Vats, S. Patel, R. Vaish, *Integrated Ferroelectr.* **2016**, *168*(1), 69-84.
[19] J. W. Stewart, J. H. Vella, W. Li, S. Fan, M. H. Mikkelsen, *Nat. Mater.* **2020**, *19*(2), 158.
[20] G. Vats, R. Vaish, C. R. Bowen, *J. Appl. Phys.* **2014**, *115*(1), 013505.
[21] G. Vats, H. S. Kushwaha, R. Vaish, *Mater. Res. Express.* **2014**, *1*(1), 015503.
[22] G. Vats, A. Chauhan, R. Vaish, *Int. J. Appl. Ceram. Technol.* **2015**, *12*, E49-E54.
[23] R. Sao, G. Vats, R. Vaish, *Ferroelectrics.* **2015**, *474*(1), 1-7.
[24] A. Chauhan, S. Patel, G. Vats, R. Vaish, *Energy Technol.* **2014**, *2*(2), 205-209.
[25] G. Vats, A. Kumar, N. Ortega, C. R. Bowen, R. S. Katiyar, *Energy Environ. Sci.* **2016**, *9*(4), 1335-1345.
[26] G. Vats, A. Kumar, N. Ortega, C. R. Bowen, R. S. Katiyar, *Energy Environ. Sci.* **2016**, *9*(7), 2383-2391.
[27] A. Waske, D. Dzekan, K. Sellschopp, D. Berger, A. Stork, K. Nielsch, S. Faehler, *Nat. Energy.* **2019**, *4*(1), 68-74.
[28] V. Srivastava, Y. Song, K. Bhatti, R. D. James, *Adv. Energy Mater.* **2011**, *1*(1), 97-104.
[29] I. M. McKinley, F. Y. Lee, L. Pilon, *Appl. Energy.* **2014**, *126*, 78-89.
[30] G. Vats, S. Patel, A. Chauhan, R. Vaish, *Int. J. Appl. Ceram. Technol.* **2015**, *12*(4), 765-770.
[31] G. Vats, Y. Bai, D. Zhang, J. Juuti, J. Seidel, *Adv. Opt. Mater.* **2019**, *7*(11), 1800858.
[32] G. Vats, J. Peräntie, J. Palosaari, J. Juuti, J. Seidel, Y. Bai, *ACS Applied Electronic Materials.* **2020**, *To be accepted after minor revision*.
[33] Z. Luo, M. Yang, M. Alexe, *ACS Applied Electronic Materials.* **2020**, *2*(2), 310-315.
[34] Z. Luo, X. Xia, M. Yang, N. R. Wilson, A. Gruverman, M. Alexe, *ACS Nano.* **2020**, *14*(1), 746-754.
[35] R. Olsen, J. Briscoe, D. Bruno, W. Butler, *Ferroelectrics.* **1981**, *38*(1-4), 975-978.
[36] R. Olsen, D. Bruno, J. Briscoe, J. Dullea, *Ferroelectrics.* **1984**, *59*(3-4), 205-219.
[37] R. Olsen, *Journal of Energy.* **1982**, *6*(2), 91-95.
[38] R. Olsen, D. Brown, *Ferroelectrics.* **1982**, *40*(1-2), 17-27.

[39] R. Olsen, D. Bruno, J. Briscoe, *J. Appl. Phys.* **1985**, *57*(11), 5036-5042.
[40] R. Olsen, D. Bruno, J. Briscoe, *J. Appl. Phys.* **1985**, *58*(12), 4709-4716.
[41] R. Olsen, D. Evans, *J. Appl. Phys.* **1983**, *54*(10), 5941-5944.
[42] H. Nguyen, A. Navid, L. Pilon, *Appl. Therm. Eng.* **2010**, *30*(14-15), 2127-2137.
[43] A. Navid, L. Pilon, *Smart Mater. Struct.* **2011**, *20*(2), 025012.
[44] I. M. McKinley, R. Kandilian, L. Pilon, *Smart Mater. Struct.* **2012**, *21*(3), 035015.
[45] F. Y. Lee, S. Goljahi, I. M. McKinley, C. S. Lynch, L. Pilon, *Smart Mater. Struct.* **2012**, *21*(2), 025021.
[46] G. Vats, *Ferroelectrics.* **2016**, *493*(1), 130-138.
[47] A. R. West, *Solid State Chemistry and its Applications*, 2nd edn., Wiley**2014**.